Improvements in Stabilisation and Cellular Structure of Al based Foams with Novel Carbonate Foaming Agent

A. Byakova[1,3], A. Sirko[1], K. Mykhalenkov[2], Yu. Milman[1], S. Gnyloskurenko[1,3,#] and T. Nakamura[3]

[1]*Institute for Problems of Materials Science, Ukrainian National Academy of Sciences,*
3 Krzhyzhanivs'ky St., 03142 Kyiv, Ukraine
[2]*NTUU "Kiev Polytechnic Institute", Peremohy ave., 37 Peremohy ave., 04056 Kyiv, Ukraine*
[3]*IMRAM, Tohoku University, 2-1-1 Katahira, Aoba-ku, Sendai 980-8577, Japan*
University, 2-1-1 Katahira, Aoba-ku, Sendai 980-8577, Japan

(Received March 29, 2006; final form April 5, 2006)

ABSTRACT

In the present paper the applicability of $CaCO_3$ foaming agent for making Al-based foams by Alporas route as well as by powder compact technique is studied. Its effect on the foaming behaviour of the melt or powder precursor, stabilisation of liquid foam with solid particles, layers or network of thin oxide films as well as on the cell size and cell wall microstructure of final solid foam is clarified and discussed in comparison with conventional TiH_2 foaming agent. It is underlined that application of the novel foaming agent is more favourable in view of the processing conditions because of remarkable improvement in foam stabilisation by melt oxidation. In addition, advantages in application of $CaCO_3$ as foaming agent for clearing the cell wall material from undesirable contaminations induced typically by conventional titanium hydride TiH_2 is justified.

Keywords: Calcium carbonate, Foaming agent, Al based foam, Foam processing route, Foam stabilisation, Cell wall microstructure

I. INTRODUCTION

The most perspective lightweight materials of cellular structure, metallic foams are characterised by multifunctional abilities due to a unique combination of physical and mechanical properties. Because of this metallic foams are of growing interest for design purposes in different sector sof industrial applications /1-3/. Closed-cell aluminium foams hold particular promise for use in automotive, railway, aerospace, and other industries in which efficient absorption of impact energy combined with beneficial thermal, acoustic, and other physical properties is important. A range of techniques was developed for making the foams among which melt processing and powder metallurgical routes are the most common. However, there is still strong incentive to develop cost effective processing routs. Moreover, processing control is also an important task to provide high quality of foams with a fine and uniform cellular structure preferably with no coarse and brittle constituents in the cell wall material /4/. At this point the Alporas route (Shinko Wire, Japan) /5/ based on the handling of a melt with calcium as the viscosity-enhancing additive and titanium hydride (TiH_2) as a gas

---

[#] Corresponding author.
E-mail: slava@tagen.tohoku.ac.jp

blowing agent holds particular promise to make machinable metal foams. In developing this method calcium carbonate ($CaCO_3$) coated by calcium fluoride (CaF_2) has been proposed by researchers in Japan /6/. Compared to titanium hydride this highly promising alternative foaming agent (FA) is cheaper and it is easier dispersed in the melt, ensuring smaller cell sizes. Performance gains in application of this promising agent for aluminium MMCs has been recently justified /7/. Usage of $CaCO_3$ as a foaming agent for production of Al-based foams via powder compact technique has not yet systematically assessed. In the present paper the applicability of $CaCO_3$ FA for making Al-based foams by the Alporas route as well as by powder compact technique is studied in detail and its role in influencing the behaviour of foaming melt and structural features of solid foam is discussed by comparing with those formulated by conventional TiH_2 foaming agent.

2. EXPERIMENTAL

2.1 Materials and experimental procedure

Both the Alporas-like route /5/ and powder compact technique were used in the foaming experiments. Titanium hydride ($TiH_{1.96}$) and calcium carbonate ($CaCO_3$) with a mean particle size of 60 μm and 8 μm, respectively, were employed as foaming agents. Powder of as received $CaCO_3$ was pre-coated by thin CaF_2-layer using the ion-exchange method /6/ to enhance wettability and provide uniform distribution of the foaming agent over the melt.

Aluminium (purity 99.95) and two commercially available aluminium alloys were used in the foaming experiments performed by the Alporas route. The casting alloy AlSi7 (similar to A356 alloy) was usually applied in foaming processes because of its low melting point and good foamability. The wrought alloy, assigned here as ZAM (similar to alloy 7075), of the chemical composition such as Al-5.5Zn-3Mg-0.6Cu-0.5Mn and doped additionally by Sc and Zr (totally 0.6 wt%) was used because of its high strength and good corrosion resistance.

Air-atomised powder of pure Al (oxygen content 0.2 wt.%) and water-atomised powder of ZAM alloy (oxygen content 0.3 wt.%) were employed in the foaming experiments being performed by powder compact technique. Particle size of powdered alloy was about 160 μm and less. Melting point and solidus temperature of the matrix Al-alloys primary determined by DTA method are given in Table 1. Both thermo-gravimetric analysis (TGA) and thermo-differential analysis (DTA) conducted in ambient atmosphere under heating rate 10 K/min were used to select processing temperature in foaming experiments with two kinds of foaming agents (TiH_2 and $CaCO_3$). Thermal history data on the onset temperature of gas evolving for both foaming agents are shown in Fig. 1. Difference in DTA tracks for the agents is attributed to strong oxidising TiH_2 powder under heating in air atmosphere.

2.1.1 Alporas route

In the first step each alloy (0.7 kg) was melted in an induction furnace under ambient atmosphere. Metallic

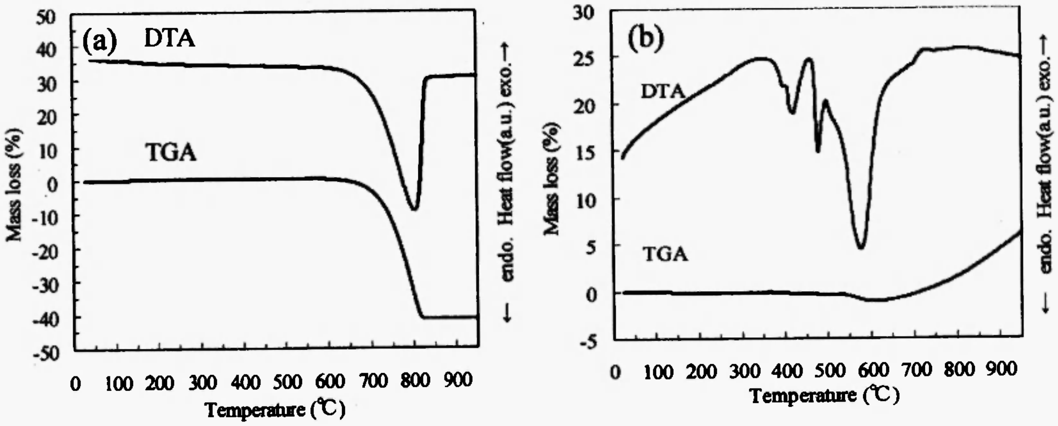

Fig. 1: TGA-DTA curves for heating (a) $CaCO_3$ and (b) TiH_2 showing the onset temperature of gas evolving.

calcium of 1 wt.% as a thickening agent was added to a melt at 750°C with vigorous stirring for 5 min, although a few experiments were conducted without Ca addition. Then, the melt was poured into a graphite crucible (85 mm i.d.) being placed in a resistance furnace and pre-heated to the required temperature. To disperse foaming agent rapidly and homogeneously throughout the melt it was added (typically 1 or 2 wt.%) to a melt under vigorous stirring with a speed being increased gradually from 700 rpm to 1000 rpm. After the specified holding time the crucible was removed from the furnace and the foam was solidify under cooling with fans. The temperature history of the melt was controlled with Pt-Pt/Rh thermocouple placed into the melt. Experimental parameters used during the foaming experiments with the Alporas route are given in Table 1.

2.1.2 Powder compact route

The powder compact route began with mixing of metal powders with powdered foaming agent. After this, the mixture was pre-compacted at room temperature to cylindrical-shaped samples with diameter, d_o, ranging from 25 to 50 mm. Foamable precursor material without any open residual porosity was prepared by rod extrusion technique at the temperature ranged from 350 to 400°C. Extrusion coefficient, k, defined by the ratio $(d_o/d_f)^2$ was varied from 15 to 85, resulting in final diameter, d_f, of the precursor material. The latter was finally foamed by heating to a temperature required by processing conditions for effective foaming (Table 2).

2.2 Structural characterisation

Foamed samples were sectioned by electro-discharge machining to examine foam quality including measurements of density, pore size and microstructural characterisation. Density was measured by weighing a sample of known volume and then relative density was defined by ratio ρ/ρ_s (where ρ and ρ_s correspond to foam density and solid density, respectively). Porosity content was derived form relation $\theta = 1-\rho/\rho_s$. Cell morphology including cell size and shape was measured by using scanned images with more than 150 cells. X-ray diffraction (XRD) analysis as well as optical and scanning electron microscopy (SEM) equipped with X-ray detectors (EDX and EPMA) were used for microstructural analysis and elementary composition of the foamed sections. Both sections prepared by machining and those impregnated with opaque epoxy were used for XRD analysis to recognise separately the phase composition of the cell wall and that of the cell face.

Table 1

Experimental parameters and mean cell sizes for Al based foams produced via Alporas route.

Matrix alloy	Al			A356			7075			
Melting point (K)	933			890			911			
Solidus temperature (K)	933			850			843			
Foaming agent	TiH_2	$CaCO_3$		TiH_2		$CaCO_3$	TiH_2		$CaCO_3$	
Ca additive (wt.%)	1	1	-	1	-	1	1	-	1	-
Foaming temperature (K)	943	948	943	923	888	953	897	903	953	953
Holding time (min)	0.5	3	3	1	0.5	2	3.5	2	6	4
Mean cell size (mm)	3.1	1.5	1.4	3	4.2	1.5	2.2	2.1	1.1	1.2

Table 2

Foaming conditions and mean cell size for Al based foams produced via powder compact route.

Matrix alloy	Al		7075	
Foaming agent	TiH_2	$CaCO_3$	TiH_2	$CaCO_3$
Foaming temperature (K)	973	1038	963	978
Mean cell size (mm)	2.2	1.2	1.9	1.1

3. RESULTS AND DISCUSSION

3.1 Alporas route

Figure 2 shows a sectional view of the samples of different Al alloys foamed with $CaCO_3$ foaming agent (a)-(c) and conventional TiH_2 agent (d)-(f). All blocks exhibit a closed-cell structure typical for Alporas foams and relative densities ρ/ρ_s ranging from 0.25 to 0.07. It is clear that a thick dense layer appears at the bottom part of the samples. Duarte and Banhart /8/ reported that appearance of such a layer is caused with melt drainage (flow downwards under gravity) followed by bubble coalescence due to the rupture of liquid cell wall. However, $CaCO_3$-foams are characterised with more uniform distribution of cells having smaller sizes than TiH_2-foams.

It is notable that $CaCO_3$ foams were obtained at higher foaming temperature and also they were held at this temperature much longer time than TiH_2-foam, as can be seen in Table 1. So, it seems that application of $CaCO_3$ foaming agent prolongs the existence of foamy melt. This could be attributed to specific features of stabilising mechanism operating in the melt foamed by $CaCO_3$ foaming agent due to melt oxidation reaction similar to that happened in FOAMCARP process investigated by Gergely *et al.* /7/.

The stabilisation mechanism for Alporas foams, especially those processed with $CaCO_3$, has not yet been discussed exhaustively in the literature. The principle mechanisms responsible for foam stability, i.e. avoidance of drainage, liquid cell wall rupture and bubble coalescence, is quite complicated and open to question. There are few theories concerning foam stability /8-11/ and the role of viscosity and surface tension of the metallic melt is under permanent dispute. Presently particle stabilisation is recognised to be a universal mechanism of metal foam stabilisation. Solid inclusions influence foam stability through their wetting behaviour (contact angle, θ of the "liquid melt-gas-solid inclusion" system), their size and shape as well as their concentration and distribution in the melt (network formation, clustering or segregations) /9,10/.

It was pointed out /9/ that for conventional Alporas route a melt viscosity is raised by factor 5 owing to finely dispersed $CaAl_2O_4$ particles being formed by oxidising Ca added to the melt and/or intermetallics,

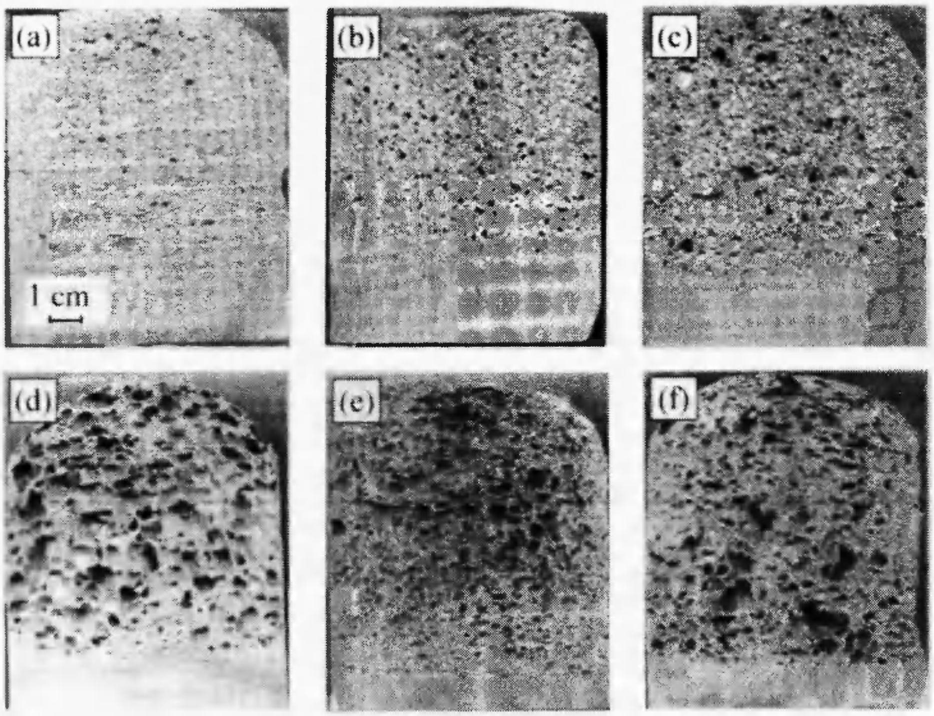

Fig. 2: Cross sectional view of the samples foamed by Alporas route of pure Al (a),(d), AlSi7 alloy (b),(e) and ZAM alloy (c),(f) processed with $CaCO_3$ (a)-(c) and TiH_2 (d)-(f) foaming agents with Ca addition to the melt.

thickening the liquid metal /3,10/. The experimental evidence given in Table 1, i.e. a combination of the foaming temperature and the holding time that results in a certain cell size, confirms the role of the solid particles in influencing the foaming process. On the one hand, reducing the foaming temperature to close or even below the melting point is required to avoid drainage and undesirable foam decay in producing TiH_2-foams without Ca additive. Gergely *et al.* /11/ state that viscosity increases with reducing the temperature close to the melting point when some fraction volume of solid phase is expected, slowing down the vertical motion of liquid. On the other hand, increasing foaming temperature results in formation of the numerous CaO oxide particles due to more complete decomposition of $CaCO_3$ and in turn increases viscosity.

Figure 3(a) shows that the surface of the cell face of $CaCO_3$-foam is covered by solid skin of Al_2O_3 oxide decorated by numerous cubic crystals of CaO oxide (A), complex oxides particles ($Ca_3Al_2O_6$ (B)) and oxide particles/films (the composition depends on the matrix alloy). In contrast to this no oxide skin appears on the cell face of TiH_2-foams and only single $AlTi_3$ particles (D) and $CaAl_4O_7$ crystals (E) are embedded in the cell wall surface (Fig. 3(b)).

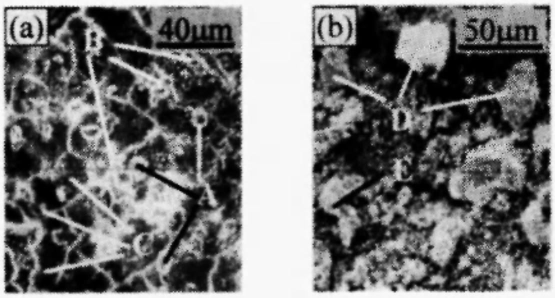

Fig. 3: SEM images of the cell faces of pure Al carbonate foam (a) and hydride foam (b).

Accumulation of CaO particles within the cell edges of $CaCO_3$-foams produced via an Alporas-like route was shown previously in Ref 12. Oxidation process is thought to convert the melt into a semi-liquid material of high viscosity, slowing down the drainage and cell coalescence. Both the foaming temperature and the cell size of $CaCO_3$-foams with and without Ca additive are quite similar (Table 1). This fact indicates the role of Ca as the thickening agent to be of little significance since its beneficial effect on the melt viscosity is probably negligible when a huge number of oxide particles appear in the melt and also a solid oxide skin is formed on the cell faces of $CaCO_3$ foams (Fig. 3(a)). The above would be essentially important in mechanical performance of the foams based on Al alloys for which the formations of brittle Ca-based intermetallic compounds are much expected. As an example, Ca additive results in formation of coarse and brittle Al_2CaSi_2 intermetallic compounds in the cell wall of Al-Si alloy foams (Fig. 4(a)).

Nonetheless, the presence of the oxide particles is obviously insufficient to elucidate the fine cellular structure of $CaCO_3$-foams. The formation of the solid oxide skin on the surface of cell faces could play a crucial role in high stability and fine cellular structure of

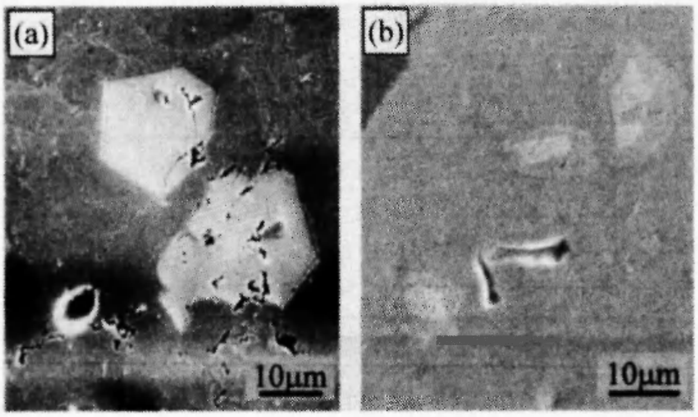

Fig. 4: SEM micrographs of Ca-based intermetallic compounds of carbonate foam (a) and Ti-rich particles of hydride foam (b) in the cell wall of Al-Si alloys.

$CaCO_3$-foams produced by the Alporas route, the same as that suggested for oxidised Cymat foams /9/ and foams produced via the FOAMCARP route /7/. It could be seen in Fig. 3(a) that solid skin of Al_2O_3 oxide (C) and of other oxides is bonded to the cell face in $CaCO_3$-foam in contrast to only a light "wool blanket" of the secondary oxides formed on the cell wall surface during solidification of TiH_2-foams [Fig. 3(b)]. It was determined by XRD analysis that the solid oxide skin created in $CaCO_3$-foams is amorphous. This skin is primarily responsible for the retention of fine cell structure in $CaCO_3$-foams, acting as prevention barrier against premature rupture of the liquid cell membranes and bubble coalescence.

In the case of hydride foam Ti-rich particles rounded by Al_3Ti layer emerge in the cell wall material (Fig. 4(b)). They are presumably the products of the partially decomposed TiH_2 foaming agent and higher temperature is required to bring the reaction to completion. No foreign inclusions are formed in the cell wall of carbonate foam in contrast to Ti-rich particles above, which is thought to impair of the cell wall ductility and toughness.

3.2 Powder compact route

A sectional view of the foamed powder compacts made with $CaCO_3$ and TiH_2 foaming agents is shown in Fig. 5. All the specimens demonstrate closed-cell structure with relative density ρ/ρ_s ranged from 0.3 to as low as 0.08. It could be seen that $CaCO_3$-foams give more uniform density distribution over the cross section and smaller cell size than TiH_2-foams, the same as it was found for Alporas foams. However, unlike Alporas foams, cells created from powder compacts exhibit elliptic shape with major axis arranged along the extrusion direction, employing the coefficient of cell shape of up to 3. Anisotropy of the cell shape increases with growing the extrusion coefficient. The powder compact technique requires higher foaming temperature compared to the Alporas route, as shown in Tables 1 and 2. It could also be seen that powder compacts with $CaCO_3$ foaming agent are foamed at higher temperature than those of TiH_2 foaming agent.

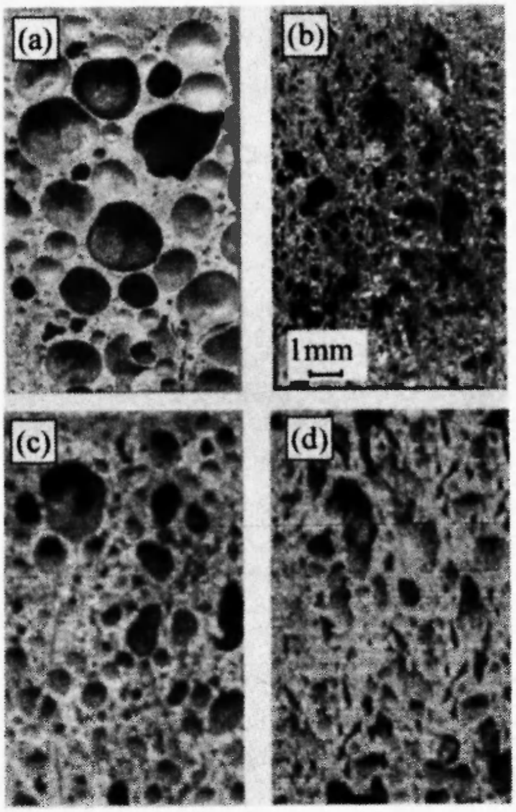

Fig. 5: Cross sectional view of PM foamed samples of pure Al (a),(b) and ZAM alloy (c),(d) processed with TiH_2 (a),(c) and $CaCO_3$ (b),(d) foaming agent.

The distinctive features above are a result of the presence of a fine network of the oxide particles over the matrix of powder compacts as shown in Fig. 6. The origin of the particles is oxygen contained by metal powder. The oxide layer is initially located on the surface of metal powder particles and, then, is broken during extrusion, leaving a fine dispersion of oxide stringers. Structures of this type have been observed /13/ in the extruded powder of MMCs, but in general they are too fine to be readily seen by SEM. Nonetheless, deformation events decorated by oxide network are clearly seen in Fig. 6.

It is clear that the oxide network acting as a mechanical barrier strongly influences the distribution of foaming agent particles, making them mostly fitted to the stringer structure. This type of structure becomes increasingly pronounced in powder compacts produced with small powder particles of $CaCO_3$ (Fig. 6(a)). Crushing the large powder particles of TiH_2 occurs under extrusion, although small particles are fitted to the oxide network (Fig. 6(b)).

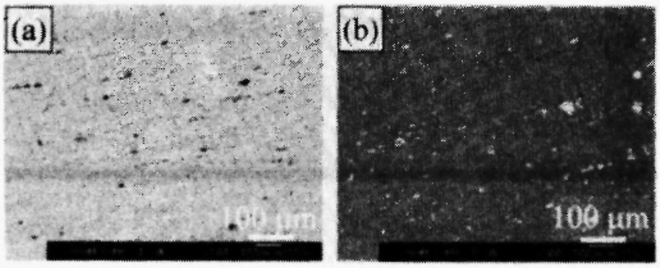

Fig. 6: SEM micrographs of ZAM alloy powder compacts of carbonate foam (a) and hydride foam (b).

During foaming these network particles survive in the melt as long as they are partially wetted by liquid metal /14/ and cannot easily move over semisolid melt. Several aspects resulting from oxide network structure in powder compacts should be mentioned here. First of all this network is considered to be an ideal mechanical barrier against cell wall thinning, providing foam stability /9,13/. That is why foaming process of powder compacts could be held under higher temperature than that for melt processing route. Furthermore, the oxidation process due to decomposition of $CaCO_3$ foaming agent produces additional oxide particles and forms of solid oxide skin on the surface of cell faces, allowing the foam to be stable with temperature increase. The second aspect concerns the effect of textured oxide network on the cell shape anisotropy in foams that increased with deformation under extrusion. Bubble nucleation and growth are probably restricted by stringer structure of the oxides network particles, although they have dynamical character in the melt due to continuous fracturing and agglomerating /13/. The next aspect relates to the fact that the network keeps the powder particles of the foaming agent in the melt, leaving their products in the cell wall material after solidification.

In summary, CaO particles are randomly scattered in the cell wall material of $CaCO_3$ foams, whereas a huge number of Al_3Ti particles together with partially reacted Ti-rich particles rounded by Al_3Ti-layers are contained in the cell wall material of TiH_2-foams. It is notable that a number of Ti-rich particles decrease with increasing deformation (extrusion coefficient k) under extrusion of the powder compacts. This fact indicates that refining the large TiH_2 particles due to their crushing under extrusion leads to greater efficiency of TiH_2 decomposition. Because of a huge number of foreign particles in the cell wall structure the foams created from powder compacts are expected to be very different from those performed by the Alporas route in terms of their associated mechanical behaviour.

4. CONCLUSION

Significant advantages in performance of Al-based foams processed by Alporas like route and powder compact technique are derived by application of coated calcium carbonate ($CaCO_3$) instead of conventional titanium hydride (TiH_2) foaming agent. The increased foam stability and fine cellular structure originates from melt oxidation due to decomposing the $CaCO_3$ foaming agent. A huge number of oxide particles causes melt viscosity to rise, slowing down foam drainage. This allows keeping stable foam at higher temperature, providing for much complete decomposition of the foaming agent and so, greater efficiency of the foaming process. In addition to this the formation of solid oxide layers on the surface of cell faces was believed to be primarily responsible for the retention of fine cellular structure in $CaCO_3$ foams, providing for effective inhibition of cell coarsening and coalescence. From this point of view the admixture of Ca as thickening agent is expected to be of little significance since its beneficial effect on the melt viscosity is likely to be negligible when a huge number of the oxide particles appear in the melt and also solid oxide skin is formed on the cell faces of $CaCO_3$ foams. This would be especially important for mechanical performance of the foams based on Al-alloys for which formation of the brittle Ca-based intermetallic compounds are much expected. Both for foams produced with Alporas and powder compact route application of $CaCO_3$ foaming agent is suggested to be favourable in view of clearing the cell wall material from undesirable brittle constituents formed usually with employing TiH_2, e.g. Ti-rich particles (residues of partially decomposed TiH_2) and/or Al_3Ti particles. As a general conclusion it could be emphasized that application of coated $CaCO_3$ as alternative foaming agent might lead to development of environmentally friendly processing routes and performance of more advanced and cheaper products.

ACKNOWLEDGEMENT

The research was partly supported by the National Academy of Sciences of Ukraine in the framework of the Project # 1.6.2.5-04 and also was fulfilled under a JSPS Fellowship Program.

REFERENCES

1. L.J. Gibson, *Annu. Rev. Mater. Sci.* **30**, 191-227 (2000).
2. L. J. Gibson and M. F. Ashby, *Cellular Solids: Structure and Properties*, Pergamon Press, New York, USA, 1988.
3. M. F. Ashby, A. G. Evans, N. A. Fleck, L.J. Gibson, et al., *Metal Foams: A Design Guide*, Butterworth – Heinemann Press, New Delhi, USA, 2000.
4. A.E. Markaki and T. W. Clyne, *Acta Mater.* **49**, 1677-1686 (2001).
5. S. Akiyama, H. Ueno, K. Imagawa, A. Kitahara, S. Nagata, K. Morimoto, T. Nishikawa and M. Itoh, US Patent, No. 4713277 (1987).
6. T. Nakamura, S. V. Gnyloskurenko, K. Sakamoto, A. V. Byakova and R. Ishikawa, *Mater. Trans.* **43**, 1191–1196 (2002).
7. V. Gergely, D.C. Curran and T. W. Clyne, *Compos. Sci. Technol.* **63**, 2301-2310 (2003).
8. I. Duarte and J. Banhart, *Acta Mater.* **48**, 2349-2362 (2000).
9. N. Babcsan, J. Banhart and D. Leitmeier, *Proc. Int. Conf. "Advanced Metallic Materials"*, Smolenice, Slovakia, 2003; 5.
10. Liqun Ma and Zhelung Song, *Scripta Mater.* **39**, 1523-1528 (1998).
11. V. Gergely, L. Jones and T.W. Clyne, *Transactions of Joining and Welding Research Institute* **30**, 371-376 (2001).
12. S. Gnyloskurenko, T. Nakamura, A. Byakova, Y. Podrezov, R. Ishikawa, and M. Maeda, *Can. Metall. Q.* **44**, 7-12 (2005).
13. C. Korner, M. Arnold and R.F. Singer, *Mat. Sci. Eng., A* 28-40 (2005).
14. R. Aveyard, B. P. Binks, J. H. Clint, and P.D.I. Fletcher, in *Foams and Emulsions* ed. by J.F. Saddoc and N. Rivier, Kluver Academic Publishers, London, UK, 1999, 21-44.